

# Determining the absolute carrier phase of a few-cycle laser pulse

P. Dietrich

*Institut für Experimentalphysik, Freie Universität Berlin, Arnimallee 14, 14195 Berlin, Germany*

F. Krausz

*Institut für Angewandte Elektronik und Quantenelektronik, Technische Universität Wien, 1040 Vienna, Austria*

P. B. Corkum

*Steacie Institute for Molecular Sciences, National Research Council, Ottawa, Ontario K1A 0R6, Canada*

Received September 20, 1999

In a strong laser field, electrons tunnel from an atom at a rate determined by the instantaneous field. If the pulse is only a few cycles in duration, the highly nonlinear nature of tunnel ionization ensures that the resultant electron wave packet is primarily formed in less than one period. Measuring the direction of above-threshold-ionization electrons produced by circularly polarized light provides a direct method of measuring the absolute carrier phase of a single pulse. The method is robust, surviving spatial and temporal integration as well as intensity fluctuations. © 2000 Optical Society of America

OCIS codes: 270.1670, 270.4180, 270.6620.

Although it is possible to produce high-power laser pulses with durations of a few periods both directly from oscillators<sup>1</sup> and by optical pulse compression,<sup>2</sup> so far the absolute carrier phase is undetermined. Changes in the carrier phase from one oscillator pulse to the next can be minimized by introduction of dispersive material inside the cavity,<sup>3</sup> but, without a method for measuring the absolute carrier phase, it is not possible to know the phase or to prevent its slow drift. We show that the absolute carrier phase can be measured by use of the angular distribution of above-threshold electrons.

Quantum mechanically, phase dependence (including sensitivity to the absolute carrier phase) arises from interference of multiple pathways to the same final state.<sup>4</sup> Only short pulses, or high-order nonlinear phenomena, permit this kind of interference from within the same pulse. High harmonic generation (HHG) is a high-order process, and its use for measuring the absolute carrier phase has been proposed.<sup>5</sup> However, HHG requires the coherent response of many atoms in a complex, ionizing environment. Therefore a dependence on the absolute carrier phase is found only for the highest harmonics and is highly sensitive to intensity fluctuations, making its use difficult.

If the pulse is short enough, high-order nonlinearities are not necessary. By selecting electrons that can be produced by two or more low-order pathways, one can observe a dependence on the absolute carrier phase.<sup>6</sup> Compared with HHG, multiphoton ionization is less complex because it is a single-atom process. Such low-order processes, however, place severe constraints on the electron spectral resolution unless the pulse is short indeed.

Here we concentrate on the single-atom above-threshold-ionization (ATI) response, using circularly polarized light. We study processes in which more

than 100 photons are absorbed, so a classical description of strong-field ionization is appropriate. We use circularly polarized light for several reasons. First, the amplitude of the electric field varies smoothly with time (Fig. 1). Therefore ionization is not modulated by the rapidly changing electric field as for linearly polarized light. Second, once it is ionized, circularly polarized light prevents electron rescattering off the parent ion.<sup>7</sup> Consequently, the direction of the above-threshold electrons is uniquely determined by the absolute carrier phase of the laser at the time of ionization.

We apply the quasi-static procedure<sup>8</sup> to describe ATI. It makes our approach intuitively clear because it naturally follows the oscillations of the electric field. The quasi-static procedure can be derived from a quantum-mechanical treatment<sup>9</sup> and has been

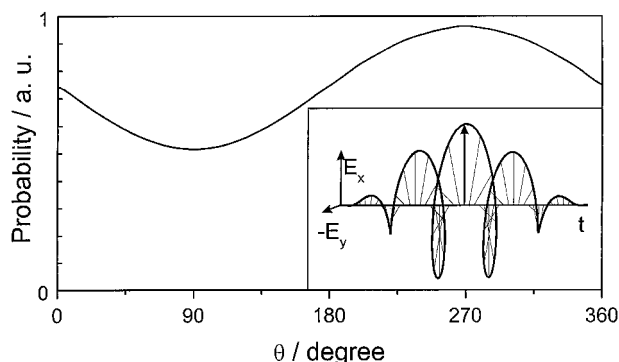


Fig. 1. Angular electron distribution for tunnel ionization of He with circularly polarized light at 800 nm with 4.8-fs duration. The absolute phase  $\phi$  was set to 0. The distribution peaks in the direction  $270^\circ \hat{=} -90^\circ$ . Inset, the time-dependent electric field vector rotating around the direction of propagation. Changing the absolute phase of the pulse will rotate the electric field so the direction at  $t = 0$  is changed.

confirmed by measurements of the ATI<sup>10</sup> and the HHG.<sup>11</sup> First we determine the probability of ionization as function of the instantaneous laser field, using Ammosov–Delone–Krainov tunneling rates.<sup>12</sup> Second, the motion of the electrons after ionization is calculated from Newton’s equations.

The final direction of the electron rotates with the electric field vector. This motion consists of a large drift in the direction 90° ahead of the electric field direction at the time of ionization and a circular component whose velocity goes to zero as the field goes to zero. For a long pulse the angular electron distribution is isotropic because tunneling is equally likely for any phase, but for short pulses significant ionization occurs during less than an optical cycle. Thus the absolute carrier phase determines the direction of the field at the moment of maximum ionization and therefore the direction of the electrons (but not the total ionization yield). Although changes in the fluence will change the total yield, for circular polarization it is possible to find conditions in which the phase dependence of the angular distribution is robust.

Figure 1 shows the angular distribution of the ATI electrons from He for a 4.8-fs pulse and a peak field of  $6 \times 10^{10} \text{ V m}^{-1}$ . We calculate the number of electrons per time step (less than  $10^{-3}$  of the optical period) brought into the continuum. Then the equations of motion for the electrons in the time-varying field  $\mathbf{E}(t) = E_{\text{env}}(t)[\mathbf{e}_x \cos(\omega t + \phi) + \mathbf{e}_y \sin(\omega t + \phi)]$  are integrated analytically with the initial condition  $v_0 = 0$ . The final velocities  $v_{x,y}(\infty) = -(e/m) \int_{t_0}^{\infty} E_{x,y}(t) dt = (e/m)[A_{x,y}(\infty) - A_{x,y}(t_0)]$  are given by the vector potential  $A$  at the time of the ionization  $t_0$  and the end of the pulse. The final angle  $\theta$  is given by  $\tan \theta = v_y(\infty)/v_x(\infty)$  (i.e.,  $\theta = 0$  corresponds to the  $x$  direction), from which we obtain the angular distribution by summing all trajectories with their respective weights that are due to the ionization probability. We use  $\phi = 0$  throughout these calculations. A change  $\Delta\phi$  of the absolute phase rotates the angular distribution by  $\Delta\phi$ . The envelope of the electric field is assumed to be  $E_{\text{env}}(t) = E_0 \cos^2(\pi t/\tau)$ , with  $t \in [-\tau/2, \tau/2]$ . The difference from a Gaussian profile in the wings of the profile is not significant because ionization occurs in the central part of the pulse. The half-width of the intensity is  $\Delta\tau \approx 0.3640\tau$ , the peak intensity is  $I_0 = \epsilon_0 c E_0^2/2$ , and the fluence of the pulse is  $F = I_0 3\tau/8$ . We characterize the angular distributions by the direction  $\theta_0$  of the angular distribution  $S(\theta)$  and by the contrast  $R_c = S_{\text{max}}/S_{\text{min}}$ . In Fig. 1 the direction is  $\theta_0 = 270^\circ$  or  $\theta_0 = -90^\circ$  and the contrast is  $R_c = 1.9$ . No spatial intensity distribution was taken into account in this example.

The solid curves in Fig. 2 represent results without spatial integration. Figure 2(a) shows the angle of the peak electric field for ionization as a function of the peak electric field for He with pulses of 4.8-fs duration (FWHM) and a center wavelength of  $\lambda = 800 \text{ nm}$ . For low fields the direction is  $-90^\circ$  and the contrast  $R_c$  is high because ionization occurs mainly during a small fraction of the pulse about the peak. With increasing intensity, ionization occurs preferentially on the rising part of the pulse, and the

direction changes [solid curve in Fig. 2(a)]. The direction of the electrons is thus a measure of the phase at which most ionization occurred. With increasing field the angular distribution also becomes more isotropic, with minimum contrast at a field where ionization starts to saturate [Fig. 2(a)]. Increasing the field further increases the contrast again because ionization is confined to an increasingly shorter part of the rising edge [solid curve in Fig. 2(b)]. From Fig. 2 we conclude that the angular electron distribution does not change with changes in the peak field for low intensities.

It is experimentally difficult to place He atoms only at the center of the laser focus, so we must treat the spatial field distribution. First, the pulses have a transverse intensity distribution that is assumed to be Gaussian. At the spatial center of a high-intensity pulse, ionization will occur before the temporal peak of the pulse. In contrast, in the wings of the radial profile, ionization occurs mainly at the temporal peak. Inasmuch as the direction of the angular distribution depends on the direction of the electric field at the time of ionization, integration over the radial intensity distribution will smear the angular distribution, thus reducing the contrast. The dashed curves in Fig. 2 show the results for the direction and the contrast after radial integration. The results are unchanged as long as the intensity is below saturation because ionization occurs only in the center of the beam.

The second effect that reduces the contrast is the intensity variation in the propagation direction. The effects are similar to the influence of a radial variation. In addition, there are phase variations of the pulse in the radial direction owing to the curvature of the focused wave fronts and axially owing to the Guoy phase. Both variations further smear the angular distribution at high intensities, and the resultant anisotropy is small (dotted curves in Fig. 2).

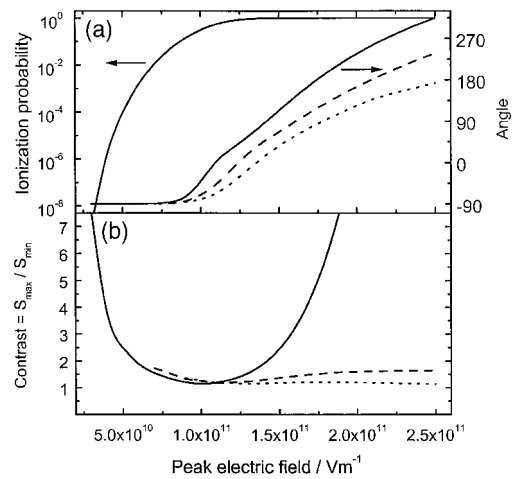


Fig. 2. (a) Direction (right-hand axis) and (b) contrast of the angular electron distribution as a function of the peak electric field for strong-field ionization of He by circularly polarized light (800 nm, 4.8 fs). The ionization probability is given in (a), left axis, without spatial integration. Solid curves, no spatial integration; dashed curves, radial integration; dotted curves, full spatial integration.

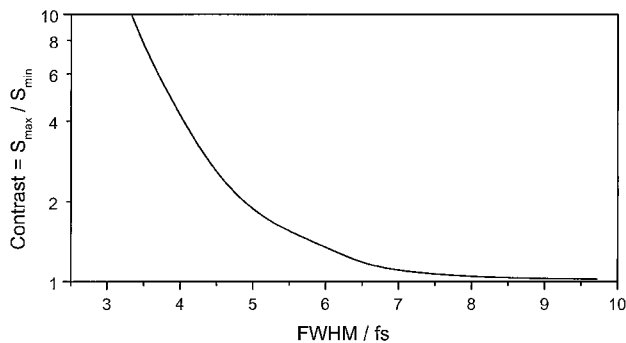


Fig. 3. Contrast of the angular electron distribution as a function of pulse duration calculated for a constant ionization yield of He ( $10^{-3}$ ).

These results suggest that the absolute carrier phase can be measured on a single-shot basis. Comparing the results in Fig. 2 shows that the optimum regime is at low fields [see Fig. 2(a)], where ionization occurs only at the peak of the field. The electron distribution is then unambiguously related to the absolute carrier phase, and amplitude fluctuations do not change the direction.

So far we have assumed state-of-the-art pulses. For longer pulses the directionality decreases because ionization occurs during a larger time interval. Figure 3 shows the dependence of the contrast on the pulse duration, calculated for an ionization yield of 0.1%. The contrast increases as the laser fluence decreases [Fig. 2(b)]. Thus for longer pulses one could use lower peak fields, but this would reduce the signal (i.e., the number of electrons). For an ionization probability of  $2 \times 10^{-6}$ , the contrast is 1.44 for a 6.3-fs pulse.

Our approach, although it is well founded, ignores some quantum-mechanical effects. We treat the electrons classically, neglecting the spatial extent of the wave function and the distribution of initial velocities. Inasmuch as we are measuring the electron distribution at macroscopic distances, the velocity distribution can lead to a blurring of the angular distribution. For small variations of the velocities  $\Delta v$  the corresponding change of the angle is  $\Delta\theta \approx \Delta v/v$ , where  $v$  is the final velocity, which scales with the electric field. The typical spreading of the electron wave function  $\Delta v$  for these cases is  $\Delta v \approx 0.7 \text{ nm/fs}$ .<sup>7,9,13</sup> Using  $v \approx 7.5 \times 10^6 \text{ m s}^{-1}$  at  $E = 10^{11} \text{ V m}^{-1}$ , we obtain  $\Delta\theta \approx 0.1$ , which is much smaller than the width of the angular distribution. The results in Fig. 2 are almost unaffected.

We emphasize the practicability of our approach. Using parameters from Ref. 14 (5-fs duration, 100- $\mu\text{J}$  energy), we can obtain a focal volume of  $6 \times 10^{-12} \text{ cm}^3$  (FWHM focal diameter,  $\approx 30 \mu\text{m}$ ) while maintaining a peak intensity of  $10^{15} \text{ W cm}^{-2}$ . Assuming a gas

density of  $10^{-3} \text{ Torr}$  (achievable in a supersonic jet expansion), there are  $10^7$  atoms in the focal volume. We can limit ionization probability to  $10^{-4}$  and still produce 1000 electrons per pulse, sufficient for single-shot electron imaging.<sup>15</sup>

In conclusion, femtosecond science aims to produce intense electric fields with almost arbitrary time structure (consistent with Maxwell's equations). Doing so requires measurement and control of the absolute carrier phase. Multiphoton ionization with circularly polarized light offers a realistic single-shot measurement method.

P. Corkum's e-mail address is paul.corkum@nrc.ca.

## References

1. J. Zhou, G. Taft, C.-P. Huang, M. M. Murnane, H. C. Kapteyn, and I. P. Christov, *Opt. Lett.* **19**, 1149 (1994); I. D. Jung, F. X. Kärtner, N. Matuschek, D. H. Sutter, F. Morier-Genoud, G. Zhang, U. Keller, V. Scheuer, M. Tilsch, and T. Tschudi, *Opt. Lett.* **22**, 1009 (1997); L. Xu, G. Tempea, Ch. Spielmann, and F. Krausz, *Opt. Lett.* **23**, 789 (1998).
2. M. Nisoli, S. DeSilvestri, O. Svelto, R. Szipöcs, K. Ferencz, Ch. Spielmann, S. Sartania, and F. Krausz, *Opt. Lett.* **22**, 522 (1997); A. Baltuka, Z. Wei, M. S. Pshenichnikov, and D. A. Wiersma, *Opt. Lett.* **22**, 102 (1997).
3. L. Xu, Ch. Spielmann, A. Poppe, T. Brabec, F. Krausz, and T. W. Hänsch, *Opt. Lett.* **21**, 2008 (1996).
4. P. Brumer and M. Shapiro, *Chem. Phys. Lett.* **126**, 541 (1986); *Annu. Rev. Phys. Chem.* **43**, 257 (1992).
5. F. Krausz, T. Brabec, M. Schnürer, and Ch. Spielmann, *Opt. Photon. News* **9**(7), 46 (1998); A. de Bohan, Ph. Antoine, D. B. Miloević, and B. Piraux, *Phys. Rev. Lett.* **81**, 1837 (1998); G. Tempea, M. Geissler, and T. Brabec, *J. Opt. Soc. Am. B* **16**, 669 (1999).
6. E. Cormier and P. Lambropoulos, *Eur. Phys. J. D* **2**, 15 (1998).
7. P. Dietrich, N. H. Burnett, M. Yu. Ivanov, and P. B. Corkum, *Phys. Rev. A* **50**, R3585 (1994).
8. P. B. Corkum, *Phys. Rev. Lett.* **71**, 1994 (1993).
9. M. Lewenstein, Ph. Balcou, M. Yu. Ivanov, A. L'Huillier, and P. B. Corkum, *Phys. Rev. A* **49**, 2117 (1994).
10. G. G. Paulus, W. Nicklich, H. Xu, P. Lambropoulos, and H. Walther, *Phys. Rev. Lett.* **72**, 2851 (1994).
11. A. L'Huillier, M. Lewenstein, P. Salières, Ph. Balcou, M. Yu. Ivanov, J. Larsson, and C. G. Wahlström, *Phys. Rev. A* **48**, R3433 (1993).
12. M. V. Ammosov, N. B. Delone, and V. Kraїnov, *Sov. Phys. JETP* **64**, 1191 (1986).
13. P. B. Corkum, N. H. Burnett, and M. Y. Ivanov, *Opt. Lett.* **19**, 1870 (1994).
14. S. Sartania, Z. Cheng, M. Lenzner, G. Tempea, Ch. Spielmann, F. Krausz, and K. Ferencz, *Opt. Lett.* **22**, 1562 (1997).
15. H. Helm, N. Bjerre, M. J. Dyer, D. L. Huestis, and M. Saeed, *Phys. Rev. Lett.* **70**, 3221 (1993).